The Korean Journal of Pathology 2012; 46: 38-41
http://dx.doi.org/10.4132/KoreanJPathol.2012.46.1.38

■ ORIGINAL ARTICLE ■

Nuclear Image Analysis Study of Neuroendocrine Tumors

Meeja Park · Taehwa Baek
Jongho Baek · Hyunjin Son
Dongwook Kang · Jooheon Kim
Hyekyung Lee

Department of Pathology, Eulji University Hospital, Eulji University School of Medicine, Daejeon, Korea

Received: August 24, 2011
Revised: December 16, 2011
Accepted: December 22, 2011

Corresponding Author
Hyekyung Lee, M.D.
Department of Pathology, Eulji University Hospital, Eulji University School of Medicine, 1306 Dunsan-dong, Seo-gu, Daejeon 302-799, Korea
Tel: +82-42-611-3460
Fax: +82-42-611-3459
E-mail: apw01@hanmail.net

Background: There is a subjective disagreement about nuclear chromatin in the field of pathology. Objective values of red, green, and blue (RGB) light intensities for nuclear chromatin can be obtained through a quantitative analysis using digital images. **Methods:** We examined 10 cases of well differentiated neuroendocrine tumors of the rectum, small cell lung carcinomas, and moderately differentiated squamous cell lung carcinomas respectively. For each case, we selected 30 representative cells and captured typical microscopic findings. Using an image analyzer, we determined the longest nuclear line profiles and obtained graph files and Excel data on RGB light intensities. We assessed the meaningful differences in graph files and Excel data among the three different tumors. **Results:** The nucleus of hematoxylin and eosin-stained tumor cells was expressed as a combination of RGB light sources. The highest intensity was from blue, whereas the lowest intensity was from green. According to the graph files, green showed the most noticeable change in the light intensity, which is consistent with the difference in standard deviations. **Conclusions:** The change in the light intensity for green has an important implication for differentiating between tumors. Specific features of the nucleus can be expressed in specific values of RGB light intensities.

Key Words: Computer-assisted image processing; Nuclear chromatin; Neuroendocrine tumors

Diagnosing malignancy is an important part of pathologists' work. In analyzing the morphologic features of malignant cells, one must first recognize abnormal features of the nucleus. The features of the nucleus indicating malignancy can be summarized as enlarged nuclei, hyperchromasia, irregularities in the nuclear membrane, coarse chromatin, and prominent nucleoli. However, there is no objective definition of abnormal features of the nucleus, and there are interobserver variations in the interpretation of such features. With recent advances in information and technology, one can substitute digital images for light microscopic findings from hematoxylin and eosin (H&E)-stained slides and translate the nuclear chromasia observed under the light microscope into a combination of red, green, and blue (RGB) light sources for digital images.[1-5] In this regard, this study obtains the objective values of RGB light intensities for digital images of well differentiated neuroendocrine tumors which show finely granular nuclear chromatin structures and compares the results with those of other tumors. To examine the irregularities in the chromatin structure, this study employs small cell carcinomas for homogeneous and least coarse chromatin structures and squamous cell carcinomas for the moderately irregular and coarse chromatin structures.

MATERIALS AND METHODS

We employed 10 cases of well differentiated neuroendocrine tumors of the rectum, 10 cases of small cell lung carcinomas, and 10 cases of moderately differentiated squamous cell lung carcinomas. We cut formalin-fixed, paraffin-embedded tissues into 3-μm sections, and stained all sections simultaneously by using H&E under standard conditions. We reviewed the slides on an Olympus BX51 microscope (Olympus Corp., Tokyo, Japan) with the 40× magnification of the apochromatic objective lens and a 0.85 numeric aperture. We maintained the same light source conditions throughout the analysis. The neuroendocrine tumors showed monotonous tumor cells with a finely granular nuclear chromatin structure on the H&E stain and positivity for neuron specific enolase, chromogranin, and synaptophysin on the immunostain. The small cell lung carcinomas showed homogeneous hyperchromatic molding nuclei, with positivity for thyroid transcription factor-1 (TTF-1), and the squamous cell lung carcinomas showed individual cell keratinization and

pISSN 1738-1843
eISSN 2092-8920

intercellular bridges, with positivity for p63. We captured digital images (1,360×1,024 pixels) of typical areas of each tumor by using an Olympus DP71 digital camera (Olympus Corp.) and saved the images in TIFF format. For each case, we selected 30 representative tumor cells that did not overlap one another and preserved clear nuclear membranes with fine chromatin. For each cell, we determined the longest line profile by using a computerized image analyzer (Image Pro program Plus ver. 6.5, Media Cybertics Co., Silver Spring, MD, USA) and obtained graph files and Excel data on RGB light intensities. For graph files, we attempted to obtain different findings for certain tumors without any clinical information. For Excel data, we obtained 30 data sets of line profiles for each case and total 900 data of line profiles were available. Each Excel data set of line profiles was composed of the values of RGB light intensities, and we analyzed a total of 2,700 data sets of RGB light intensities obtained from the 900 data sets of line profiles. We measured the mean and standard deviation (SD) of RGB light intensities for line profiles for each type of tumor. For statistical analyses, we conducted an ANOVA and considered $p<0.05$ to be significant.

RESULTS

We expressed the purple color of the nuclei of H&E stained tumor cells as a combination of RGB light sources. Among these light sources, blue provided the highest intensity, whereas green, the lowest intensity. In each case, the patterns and values of means and SDs of RGB light intensities for the 30 cells varied (Table 1). There were significant differences in RGB light intensities among well differentiated neuroendocrine tumors of the rectum, small cell lung carcinomas, and squamous cell lung carcinomas (Table 2).

In terms of graph files, small cell lung carcinomas showed a relatively flat pattern of RGB light intensities (Fig. 1A). However, with increased irregularities in chromatin in neuroendocrine tumors and squamous cell carcinomas, green showed discordant fluctuations in light intensities, and red and blue showed generally similar patterns (Fig. 1B, C). In terms of the differentiation between the three types of tumors, the change in the light intensity for green was the most meaningful result for graph files, and this may be related to the significant difference in SDs of light intensities for green based on Excel data.

DISCUSSION

Recognizing various features of the nucleus is an important part of cellular pathology. Some tumors show specific diagnostic features of the nucleus, such as ground glass nuclei or salt pepper nuclei. However, because of a lack of correlations be-

Table 1. Means and standard deviations of RGB light intensities in each case of neuroendocrine tumors, small cell carcinomas, and squamous cell carcinomas

Case No.	Neuroendocrine tumor			Small cell carcinoma			Squamous cell carcinoma		
	Red	Green	Blue	Red	Green	Blue	Red	Green	Blue
1	170.03±3.77	76.88±6.86	190.76±1.69	132.54±10.63	25.56±10.63	156.61±9.39	173.00±7.36	74.31±13.39	183.14±4.88
2	174.59±6.67	93.03±5.63	194.05±3.81	161.64±10.47	54.20±10.47	183.30±5.33	169.72±5.71	83.09±11.04	182.98±3.46
3	169.49±5.27	76.78±14.43	192.30±2.77	143.95±10.55	39.58±10.55	166.86±9.30	171.96±5.70	78.08±13.35	178.13±5.37
4	170.16±4.00	89.00±11.24	194.58±2.54	140.64±14.28	30.32±8.62	164.03±9.94	167.07±6.45	78.52±13.26	182.53±4.01
5	175.37±4.46	86.63±10.70	194.93±2.37	146.82±10.03	33.08±8.07	162.96±7.46	171.89±5.59	73.61±10.60	180.22±4.36
6	161.59±5.34	72.13±9.67	184.73±3.34	155.03±13.01	44.22±9.37	171.20±9.02	172.98±6.51	82.24±11.40	178.99±4.48
7	174.29±6.13	89.12±12.28	192.93±3.71	135.21±10.90	37.34±7.14	152.88±8.42	174.42±5.29	108.04±12.78	186.18±3.83
8	175.93±4.58	79.75±11.68	190.00±3.37	141.63±11.88	42.30±9.69	143.45±7.89	168.60±8.01	84.85±15.49	183.06±4.83
9	145.73±7.60	40.33±7.85	171.12±5.23	151.05±9.72	41.84±8.74	148.48±7.32	166.64±9.00	69.88±15.85	174.70±6.50
10	181.87±4.88	129.00±11.55	185.06±3.47	154.96±8.38	55.16±12.30	165.25±5.39	159.11±7.12	72.68±12.79	172.08±4.34

RGB, red, green, and blue.

Table 2. Comparison of RGB light intensities among three tumor groups

	Red	p-value	Green	p-value	Blue	p-value
NET	169.91±10.91	<0.001	83.27±23.70	<0.001	189.05±7.66	<0.001
SCC	169.54±7.93		80.53±16.50		180.20±6.17	
SqCC	146.35±14.41		40.36±13.12		161.50±13.61	

Data shown as mean±standard deviation. A one-way analysis of variance (ANOVA) is used for comparing the parameters for multiple groups.
The p-value< 0.05 is considered to be significant.
RGB, red, green, and blue; NET, neuroendocrine tumor; SCC, small cell carcinoma; SqCC, squamous cell carcinoma.

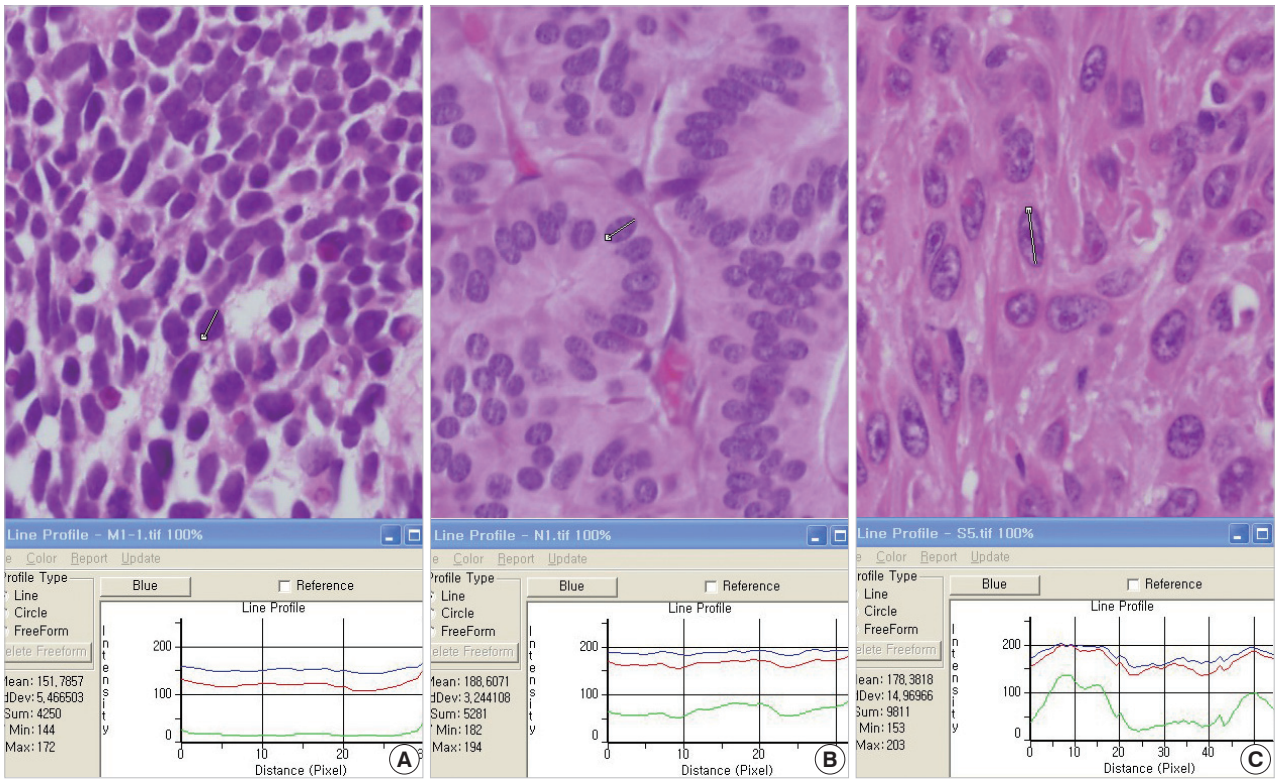

Fig. 1. Graph files of (A) small cell carcinoma, (B) neuroendocrine tumor, and (C) squamous cell carcinoma.

tween descriptive terms and reproducible objective values of the nucleus, there is some interobserver discrepancy in the interpretation of various features of the nucleus. Recently, with the development of quantitative pathology based on digital images, nuclear features can be quantified based on relatively objective values. This has opened a new era in which image analysis tools may enhance reproducibility in the interpretation of morphologic findings, complementing subjective assessments by researchers. This idea has already been incorporated into many automated instruments.[6,7]

A number of studies have provided quantitative estimates of various parameters of the nucleus, including its area and volume, the size of nucleolus, and mitosis, and demonstrated some correlations between such parameters and biological activity. However, few studies have focused on nuclear chromasia.[8-12] Recognizing that all colors in a digital image reflect some RGB combination and that digital images can be converted into numerical values of RGB light intensities, we examined the difference in light intensities between three types of tumors. The results indicate that the highest intensity was from blue, whereas the lowest intensity was from green. This may be because the purple color of the H&E stain is a mixture of blue and red with more blue than red.

We compared the results for graph files with those by Excel data and found that the SD of light intensities for green seemed to be responsible for the change in light intensities for green in graph files. Because the SD indirectly indicates how different from the mean value, the irregularities in hyperchromatic and hypochromatic patterns of the nucleus may be related to SD, not to the mean. In this study, we evaluated the data by considering only means and SDs simply, later a kind of mathematical function relation using values of RGB light intensities stressing the SD would be an important factor in the recognition of abnormal chromatin.

Different values of RGB light intensities for a particular tumor may be due to differences in the proportion of the dye complex with the cellular molecules along the different levels of tissue sections in a three dimensional cell. When we reviewed the results of graph files and Excel data on light intensities for line profiles, the graph files were better than Excel data in terms of the visual perception of differences within short time because the graph files provided three line graphs of light intensities simultaneously.

Digital images are not free of artifacts. It is not possible to have an image that is completely free of some form of processing. Although digital images are nearly the same as images from

 http://dx.doi.org/10.4132/KoreanJPathol.2012.46.1.38

35 mm film, a number of factors can influence the quality of digital images, including the thickness of tissue, the status of the lens of the light microscope/camera, and the dye condition.[13] Under such conditions, Pritt *et al.*[14] provided some guidelines for digital imaging for pathology, and we considered the importance of reference values for quality assurance in the interpretation of digital images. Thus, with additional experience and knowledge, the "salt and pepper" and "ground glass" features of the nucleus may be expressed in specific values of RGB light intensities based on reference control images. In addition, we can develop some functional formula by using the values of light intensities corresponding to meaningful chromatin clumping and employ them to enhance the reading power of automated screening instruments.

Conflicts of Interest

No potential conflict of interest relevant to this article was reported.

REFERENCES

1. Wilbur DC. Digital cytology: current state of the art and prospects for the future. Acta Cytol 2011; 55: 227-38.
2. Pinco J, Goulart RA, Otis CN, Garb J, Pantanowitz L. Impact of digital image manipulation in cytology. Arch Pathol Lab Med 2009; 133: 57-61.
3. Barshack I, Kopolovic J, Malik Z, Rothmann C. Spectral morphometric characterization of breast carcinoma cells. Br J Cancer 1999; 79: 1613-9.
4. Stenkvist B, Westman-Naeser S, Holmquist J, *et al.* Computerized nuclear morphometry as an objective method for characterizing human cancer cell populations. Cancer Res 1978; 38: 4688-97.
5. Wells WA, Rainer RO, Memoli VA. Basic principles of image processing. Am J Clin Pathol 1992; 98: 493-501.
6. Wilbur DC, Prey MU, Miller WM, Pawlick GF, Colgan TJ. The AutoPap system for primary screening in cervical cytology: comparing the results of a prospective, intended-use study with routine manual practice. Acta Cytol 1998; 42: 214-20.
7. Kayser K, Görtler J, Goldmann T, Vollmer E, Hufnagl P, Kayser G. Image standards in tissue-based diagnosis (diagnostic surgical pathology). Diagn Pathol 2008; 3: 17.
8. Komitowski D, Janson C. Quantitative features of chromatin structure in the prognosis of breast cancer. Cancer 1990; 65: 2725-30.
9. Pienta KJ, Coffey DS. Correlation of nuclear morphometry with progression of breast cancer. Cancer 1991; 68: 2012-6.
10. Bartels PH, Montironi R, Hamilton PW, Thompson D, Vaught L, Bartels HG. Nuclear chromatin texture in prostatic lesions. II. PIN and malignancy associated changes. Anal Quant Cytol Histol 1998; 20: 397-406.
11. Bartels PH, Montironi R, Hamilton PW, Thompson D, Vaught L, Bartels HG. Nuclear chromatin texture in prostatic lesions. I. PIN and adenocarcinoma. Anal Quant Cytol Histol 1998; 20: 389-96.
12. Bartels PH, da Silva VD, Montironi R, *et al.* Chromatin texture signatures in nuclei from prostate lesions. Anal Quant Cytol Histol 1998; 20: 407-16.
13. Mulrane L, Rexhepaj E, Penney S, Callanan JJ, Gallagher WM. Automated image analysis in histopathology: a valuable tool in medical diagnostics. Expert Rev Mol Diagn 2008; 8: 707-25.
14. Pritt BS, Gibson PC, Cooper K. Digital imaging guidelines for pathology: a proposal for general and academic use. Adv Anat Pathol 2003; 10: 96-100.